KRas-ERK signalling promotes the onset and maintenance of uveal melanoma through regulating JMJD6-mediated H2A.X phosphorylation at tyrosine 39

Yaping Li, Peng Yu, Ying Zou, Wenrui Cai, Weixuan Sun & Ning Han

Taylor & Francis
Taylor & Francis Group

KRas-ERK signalling promotes the onset and maintenance of uveal melanoma through regulating JMJD6-mediated H2A.X phosphorylation at tyrosine 39

Yaping Li[a], Peng Yu[a], Ying Zou[a], Wenrui Cai[a], Weixuan Sun[b] (iD) and Ning Han[a]

[a]Department of Ophthalmology, The Second Hospital of Jilin University, Changchun, PR China; [b]Department of Gastrointestinal Colorectal and Anal Surgery, China-Japan Union Hospital of Jilin University, Changchun, PR China

ABSTRACT

Since DNA damage is a first incident occurred during a tumour attack, it is rational that histone H2A.X phosphorylation on tyrosine 39 (H2A.X^{Y39ph}) may act as a tumour-relevant factor. This study was aimed to test the authenticity of the hypothesis. Uveal melanoma MP65 cells were transfected for expression of KRas mutated. H2A.X phosphorylation and ERK1/2 was measured, and transwell experiment was performed to examine the consequents of H2A.X^{Y39ph} on MP65 cells developing and migration. Regulatory relationship between H2A.X^{Y39ph} and ERK1/2 downstream genes were measured. Moreover, whether JMJD6 and MDM2 are involved in H2A.X phosphorylation was studied. Mutation of Ras activated ERK1/2 signalling and inhibited H2A.X phosphorylation at Y39. Silence of H2A.X^{Y39ph} contributed to the regulation of MP65 cells growth, migration and transcription of ERK1/2 downstream genes, including CYR61, IGFBP3, WNT16B, NT5E, GDF15 and CARD16. The repressed H2A.X phosphorylation through Ras-ERK1/2 signalling might be through MDM2-mediated JMJD6 degradation. Our study suggested that Ras-ERK1/2 signalling inhibited H2A.X phosphorylation at Y39, which led to the uncontrolled developing and migration of uveal melanoma cells. In addition, H2A.X phosphorylation was mediated possibly through JMJD6 which could be degraded by MDM2.

Introduction

Uveal melanoma is a serious original intraocular malignance in adults with the age ranged from 40 to 50 years old. To date, many miscellaneous treatments have been recommended in clinic to manage this cancer, like eye enucleation, radiation therapy and transpupillary thermotherapy, but these therapies mainly focused on the local treatment of the eyeball instead of the status of metastatic patients [1]. Based on these reasons, a better understanding of uveal melanoma is still required which will be helpful for further development of novel treatment strategies. There are several host susceptibility factors being recognized to be related to the maintenance of this cancer, including light eye colour, Caucasian race, the ability to tan and fair skin [2]. Apart from them, Ras-ERK activation has been suggested as a mechanism of uveal melanoma cell proliferation and malignant transformation [3]. Inhibition of ERK signalling was shown in trials to exert limited clinical benefits for uveal melanoma [4]. The above researches collectively revealed the involvement of ERK1/2 signalling in the maintenance of uveal melanoma. However, the mechanism is still unclear.

Epigenetics is a science that studies the change of heritable phenotype, while the DNA sequence of the genome is unaltered. The heritable phenotype changes mainly comprise histone modification, DNA methylation and non-coding RNA regulation [3]. There are five subtypes of histone: H1, H2A, H2B, H3 and H4. It has been mentioned that histone modification is an epigenetic mechanism that is closely associated with carcinogenesis [5]. H2A.X, an element of histone H2A family, locates downstream of the DNA damage kinase signalling cascade [6]. Histone H2A.X phosphorylation on serine 139, also called γ-H2A.X, is a key indicator of DNA damage [7]. It has been proved that histone H2A.X on tyrosine 39 (H2A.X^{Y39ph}) is a prerequisite for γ-H2A.X formation [8]. While recent studies have pointed out that H2A.X has a tumour suppressive function by avoiding genome unstablity and acts as a biomarker for detecting DNA damage during therapy [9,10], the exact function of H2A.X^{Y39ph} in cancer is still unclear.

To this end, this study attempted to reveal the role of H2A.X^{Y39ph} in uveal melanoma MP65 cells. This study demonstrated that H2A.X^{Y39ph} could be specifically down-regulated by Ras-ERK1/2 signalling, and H2A.X^{Y39ph} was involved in MP65 cells phenotypes. It has been well-known that JMJD6 possesses a demethylase activity both on histone and tumourigenesis [11]. JMJD6 exerts intrinsic tyrosine kinase activity and use ATP and GTP as phosphate donators to phosphorylate site Y39 of H2A.X [12]. Therefore, we focused

on investigation JMJD6 in order to explain the anti-tumour activities of H2A.X^{Y39ph}.

Materials and methods

Plasmids

The full-length cDNAs of wild type of KRas (Ras-WT), H4, JMJD6 and MDM2 were made through PCR and inserted into pEGFP-N1 plasmid (Clontech Inc., Palo Alto, CA) and HA-tag vector (Invitrogen, Carlsbad, CA). pEGFP-KRas$^{G12D\ T35S}$ construct was mutated through site-directed mutagenesis. A siRNA specific for MDM2 (si-MDM2) was obtained from GenePharma (Shanghai, China). The pEGFP-H2A.X^{Y39A} construct was constructed through the TaKaRa MutanBEST Kit (TaKaRa, Dalian, China).

Cell

MP65 cells got from American Type Culture Collection (ATCC; Manassas, VA) were put in 90% DMEM medium (Sigma-Aldrich, St. Louis, MO, USA) and 10% fetal bovine serum (FBS; Hyclone, Logan, UT). The cells were kept at 37 °C in a wet incubator with 95% air and 5% CO_2.

Transfection

Transfection was carried out in 6-well plates by using Lipofectamine 2000 (Invitrogen, Carlsbad, CA, USA) as recommended by the manufacturer. MP65 cells were put in 6-well plates for adherence. When the cells were grown to 50%~60% confluence, transfections were done. Transfection was stopped by changing culture medium after 48 h, qPCR or Western blot was employed to examine transfection efficiency.

qRT-PCR

RNA was collected from cells by TRIzol reagent (Invitrogen, Carlsbad, CA, USA). Five micrograms of total RNA from every sample was subjected to reverse transcription through M-MuLV reverse transcriptase (Invitrogen, Carlsbad, CA, USA). qPCR was carried out in triplicate through QuantiTect SYBR Green PCR Kit (Qiagen, Hilden, Germany). Consequents were normalized to GAPDH expression and relative expression was computed according to the $2^{-\Delta\Delta Ct}$ way [13].

Cell viability

The transfected MP65 cells (5×10^3 cells/well) were put in 96-well plates. 3-(4,5-Dimethylthiazol-2-yl)-2 5-diphenyl-2Htetrazolium bromide solution (MTT; Sigma-Aldrich, St. Louis, MO, USA) with final concentration of 5 mg/mL was added into every well after 48 h incubation. Plates were kept for 4 h, and then 150 μL dimethyl sulphoxide (DMSO; Sigma-Aldrich, St. Louis, MO, USA) was used to dissolve the formazan crystals. The plates were placed in a microplate reader (Bio-Rad, Hercules, CA, USA), and were shaken for 10 min.

Absorbance (OD-value) was recorded at a wavelength of 490 nm.

Soft-agar colony formation experiment

DMEM medium containing 6 g/L agarose (Invitrogen, Carlsbad, CA) was added in 24 well plates (1 mL per well), and plates were put for 30 min at 4 °C. The transfected MP65 cells resuspended in DMEM medium including 3.5 g/L agarose were put in 24-well plates. Final concentration of the cells was 1×10^6 cells/L. Colonies were recorded microscopically after 2 weeks incubation at 37 °C.

Migration experiment

A transwell chamber with 8-μm pore filters (Costar, Boston, MA) was used for the measurement of MP65 cells migration. The upper chamber was kept with 1×10^4 MP65 cells in non-serum culture medium and lower chamber was kept with full medium. Cells in the upper side were removed after 24 cultivation at 37 °C and cells in the lower side was treated with methanol, stained with 0.5% crystal violet (Beyotime, Shanghai, China) and OD-values were recorded through microplate reader at 570 nm.

Flow cytometric analysis

The transfected MP65 cells in 6-well plates were gathered and cleaned twice with phosphate-buffered saline (PBS; Beyotime, Shanghai, China). Cells were then treated with chilled 70% ethanol in the whole night at 4 °C. Cells were incubated with the solution including 50 μg/mL propidium iodide (P; Invitrogen, Carlsbad, CA, USA), Triton X-100 (0.1%) and RNase A (20 μg/mL) in room for 30 min. A FACS scan (Becton Dickson, San Jose, CA, USA) was used to get results. Cell distribution in G0/G1, S and G2/M phases was analysed by ModFit software (Verity Software House, Topsham, ME, USA).

Western blot analysis

Protein was got through RIPA lysis buffer (Beyotime, Shanghai, China) and was examined through BCA Protein Assay Kit (Solarbio, Beijing, China). Protein samples were isolated through SDS-PAGE and the separated proteins were transferred onto PVDF membranes (Beyotime, Shanghai, China). After blocking in BSA-TBST solution in the room for 1 h, membranes were cultured with specific primary antibodies overnight at 4 °C. The membranes were then incubated with HRP-conjugated secondary antibodies in room for 1 h, and Western Blotting Luminol Reagent (Santa Cruz Biotechnology, CA, USA) was employed to get positive blots. Image Lab^{TM} Software (Bio-Rad, Hercules, CA, USA) was employed to get bands.
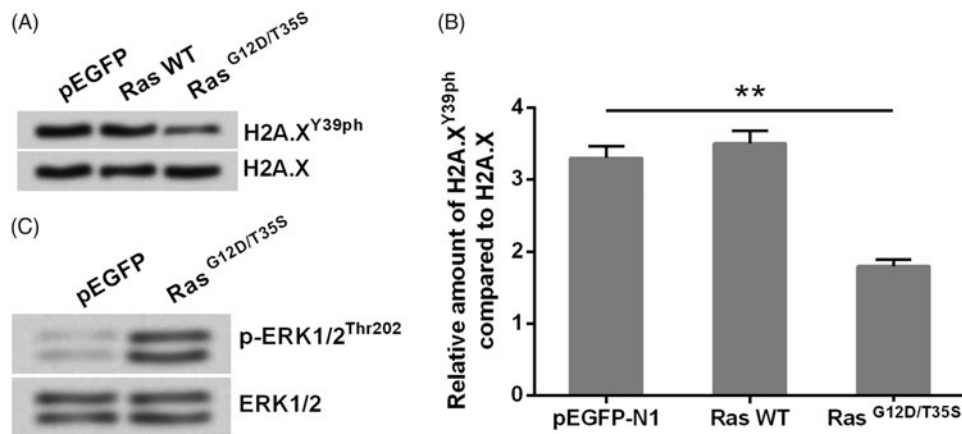
Figure 1. H2A.X^{Y39ph} was regulated via Ras-ERK1/2 signalling. MP65 cells were transfected with pEGFP-N1 vector (an empty plasmid), Ras$^{G12D/T35S}$ plasmid, or Ras WT plasmid. H2A.X^{Y39ph} expression was examined through (A) Western blot followed by (B) densitometry analysis. **$p < .01$ ($n = 3$), pEGFP-N1 versus Ras$^{G12D/T35S}$. (C) ERK1/2 expression was measured by Western blot.

Chromatin immunoprecipitation (ChIP)

The transfected cells were fixed with 1% formaldehyde in the room for 10 min for crosslinking. To finish the crosslinking, 1 M glycine was added into the sample and incubated in the room for 5 min. After washing twice with ice-cold PBS, cells were collected and lysed with SDS Lysis Buffer (Beyotime, Shanghai, China). Lysates were sonicated in an ultrasonic bath (Ultrasonic Processor VCX-750, 25% power, 4.5 s impact, 9 s gap). Then, centrifuge samples at 10,000 g at 4 °C. Then, 100 μL supernants were blended with 900 μL ChIP Dilution Buffer (Beyotime, Shanghai, China), input 200 μL mixed solution and the rest solution was incubated with Protein A + G Agarose/Salmon Sperm DNA (Beyotime, Shanghai, China) at 4 °C for 30 min. Immunoprecipitation was carried out by using anti-H2A.X^{Y39ph} antibody (Code No.: H5110-08C, United States Biological, Salem, MA,USA) and anti-JMJD6 antibody (Code No.: 33079, Signalway Antibody LLC, College Park, MD, USA), anti-IgG antibody (Code No.: ab171870, Abcam, Cambridge, MA, USA) served as a comparison. The beads were cleaned as previously described [14] and lots of immunoprecipitated DNA and input DNA were analysed by qRT-PCR.

Statistical analysis

Consequents were revealed as mean ± SD. SPSS version 19.0 software (IBM, Armonk, NY) was employed to analyse data. Difference between sets was analysed through one way ANOVA followed by Duncan post-hoc multiple comparisons. A notable consequent was p values of <.05.

Results

Ras-ERK1/2 signalling regulated H2A.X^{Y39ph}

Figure 1(A,B) indicated that the relative amount of H2A.X^{Y39ph} compared with H2A.X was significantly declined in Ras$^{G12D/T35S}$ set, contrasted with pEGFP set ($p < .01$), indicating Ras point mutations suppressed the phosphorylation of H2A.X at Y39. Besides, Western blot analytical results indicated that ERK1/2 signalling was remarkably actuated in

Ras$^{G12D/T35S}$ group as compared to pEGFP group (Figure 1(C)), suggesting Ras worked as a switch to activate ERK1/2 signalling, which was consistent with previous studies [15,16]. These data linked Ras-ERK1/2 signalling with the phosphorylation of H2A.X.
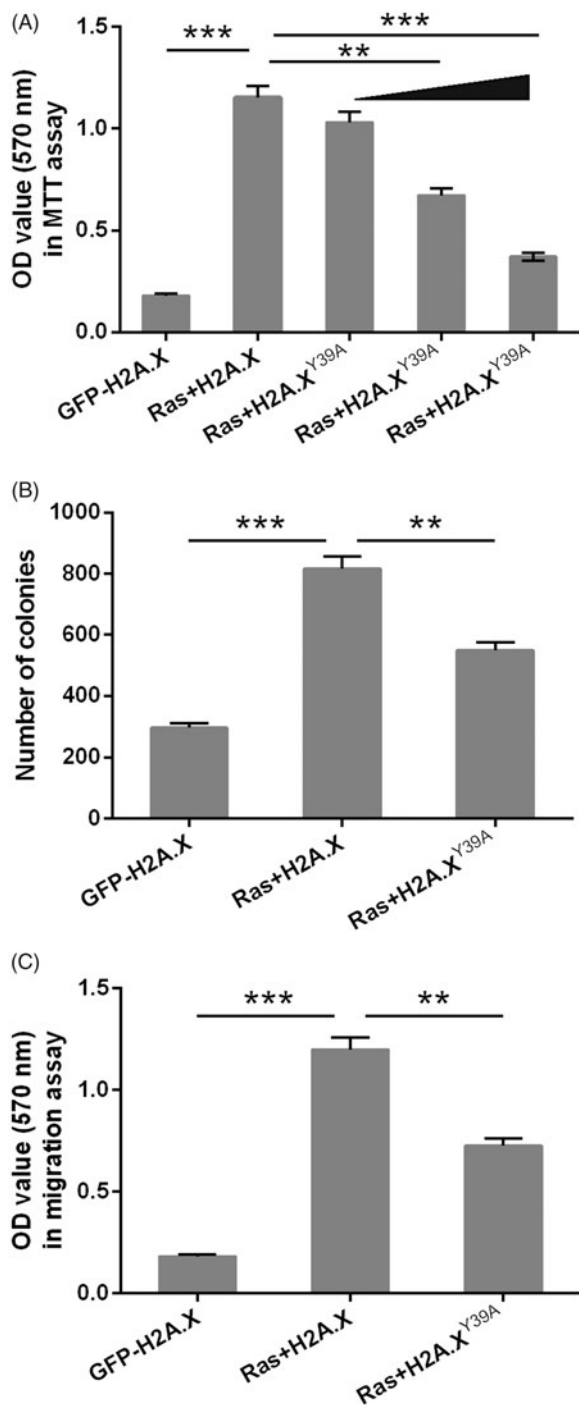
Silence of H2A.X^{Y39ph} contributed to the regulation of uveal melanoma cell phenotypes

Next, H2A.X^{Y39A} plasmids were employed to simulate the phosphorylated H2A.X and plasmids were co-transfected with Ras$^{G12D/T35S}$ into MP65 cells. MTT experiment indicated that OD values in cells co-transfected with plasmids expressing Ras$^{G12D/T35S}$ and H2A.X were significantly increased compared with those in the cells transfected with H2A.X plasmid alone (Figure 2(A), p<.001), suggesting activation of ERK1/2 signalling promoted cell viability. Moreover, we found that phosphorylation of H2A.X could significantly inhibit MP65 cells viability. Cell activity was gradually decreased by transfection with the plasmids for expression of Ras$^{G12D/T35S}$ and H2A.X^{Y39A} contrasted with those transfected with the plasmids for expression of Ras$^{G12D/T35S}$ and H2A.X ($p < .01$ or <.001). Figure 2(B,C) indicated the similar trends that colonies number and OD-values in migration experiment were both raised in Ras + H2A.X set, contrasted with GFP-H2A.X set ($p < .001$). However, they were cut down in Ras + H2A.X^{Y39A} set contrasted with Ras + H2A.X set ($p < .01$). These data collectively suggested that phosphorylation of H2A.X partially inhibited the promotion consequents of Ras-ERK1/2 on MP65 cells developing and migration.

H2A.X^{Y39ph} modulated the transcription of ERK1/2 downstream genes

Figure 3(A) indicated that RNA levels of CYR61 ($p < .01$), IGFBP3 ($p < .01$) and WNT16B ($p < .001$) were notably increased, whereas RNA levels of NT5E ($p < .01$), GDF15 ($p < .001$) and CARD16 ($p < .001$) were notably decreased in Ras + H2A.X set, contrasted with GFP + H2A.X set. Of note, altered expression of these genes by Ras mutated at G12D and T35S was attenuated by H2A.X^{Y39A} ($p < .05$ or <.01). ChIP

Figure 2. Silence of H2A.X^{Y39ph} contributed to the regulation of uveal melanoma cell phenotypes. pEGFP-H2A.X, Ras$^{G12D/T35S}$ plasmid, or increasing amounts of H2A.X^{Y39A} plasmid (0.5, 1, and 2 g) were transfected into MP65 cells. H2A.XY39A plasmids were constructed to mimic H2A.X^{Y39ph}. (A) OD values in MTT assay reflected cell viability. (B) Colonies numbers were measured through soft-agar colony formation experiment. (C) OD values in Transwell assay reflected cell migration. **$p < .01$, Ras + H2A.X versus Ras + H2A.X^{Y39A}, ***$p < .001$ ($n = 3$).

assay results indicated that the abundance of H2A.X^{Y39} was cut down at promoters of these genes ($p < .001$, Figure 3(B)) with Ras-ERK1/2 activation. Thus, we inferred that the transcription of ERK1/2 downstream genes could be modulated through H2A.X phosphorylation at Y39.

Overexpression of JMJD6 recovered H2A.X^{Y39ph} expression and uveal melanoma cell phenotypes

Considering JMJD6 is a main molecular kinase for H2A.X^{Y39ph}, the following study investigated the involvement of JMJD6 in H2A.X^{Y39ph}-mediated uveal melanoma cell phenotypes. First, JMJD6 expression in MP65 cells was overexpressed by transfection. Transfection efficiency was examined through Western blot, and results in Figure 4(A) showed that JMJD6 was successfully overexpressed post-transfection. Then, we found that JMJD6 overexpression recovered H2A.X^{Y39ph} expression which was down-regulated by Ras point mutation (Figure 4(B)). Furthermore, data in Figure 4(C–E) showed that JMJD6 exhibited H2A.X^{Y39ph}-like effects in regulating MP65 cells viability, migration and cell-cycle progression. As compared to Ras + pCMV group, cell activity ($p < .05$ or $< .001$), migration ($p < .05$ or $< .001$) and the rate in S phase were all declined in Ras + JMJD6 group.

Activation of ERK1/2 induced the degradation of JMJD6 and led to the down-regulation of H2A.X^{Y39ph}

Furthermore, we tried to decode the regulatory relationship between JMJD6 and ERK1/2 signalling. Figure 5(A) showed that the mRNA level of JMJD6 was unaffected by Ras point mutation; i.e. ERK1/2 activation cannot affect the pre-transcription level of JMJD6. However, ERK1/2 activation remarkably down-regulated the pro-transcriptional protein level of JMJD6 (Figure 5(B)). Besides, the down-regulation of JMJD6 and H2A.X^{Y39ph} by ERK1/2 activation occurred simultaneously (Figure 5(C)). ChIP assay was employed to see if JMJD6 was related to ERK1/2 downstream genes' transcription. Figure 5(D) indicated that the enrichment of JMJD6 was significantly declined at promoters of these genes ($p < .05$, $< .01$ or $< .001$) with Ras-ERK1/2 activation, indicating JMJD6 could regulate ERK1/2 downstream genes' transcription. Next, MP65 cells were treated by MG132, an inhibitor of proteasome, to check if JMJD6 modulated H2A.X^{Y39ph} post-transcriptionally. Figure 5(E) indicated that JMJD6 protein level was recovered to the baseline by MG132 treatment in Ras$^{G12D/T35S}$ transfected cells. Figure 5(F) indicated that H2A.X^{Y39ph} standards were remarkably decreased through Ras$^{G12D/T35S}$ after 48 h of transfection without MG132. 25 μM MG132 could recover H2A.X^{Y39ph} levels (Figure 5(G)). Altogether, Ras-ERK1/2 signalling inhibited H2A.X phosphorylation via post-transcriptional regulation of JMJD6.

Activation of ERK1/2 degraded JMJD6 via modulation of MDM2

Finally, we studied whether ERK1/2 degraded JMJD6 via modulation of E3 ubiquitin ligase MDM2. Figure 6(A) showed that transfection with MDM2-His apparently up-regulated MDM2 expression in MP65 cells, but reduced the expression of JMJD6. This phenomenon was also confirmed in Figure 6(B). However, JMJD6 level could not be down-regulated by MDM2 mutated type (Figure 6(C,D)), which preliminary draw a conclusion that MDM2 was essential for JMJD6 degradation. Subsequently, Figure 6(E) indicated that ERK1/2
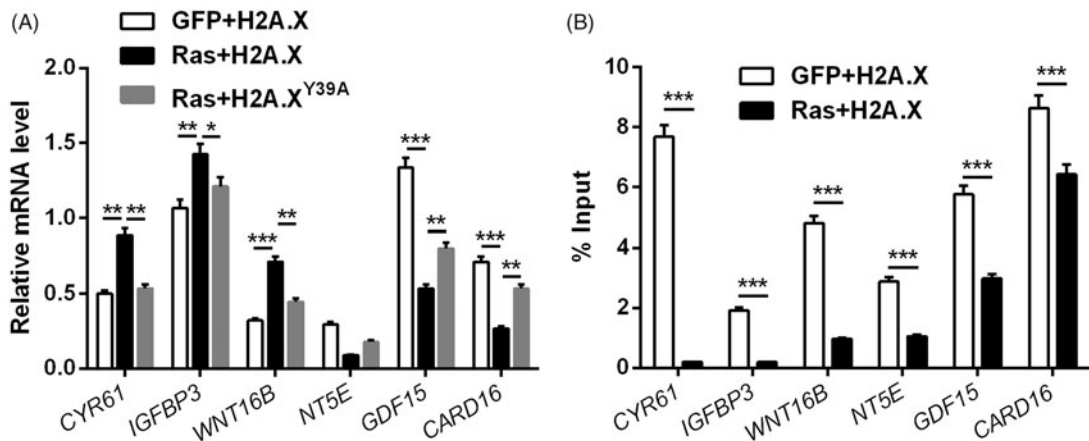
Figure 3. H2A.X^{Y39ph} modulated ERK1/2 downstream genes' transcription. (A) RNA levels of several genes were tested through qRT-PCR after transfection with pEGFP-H2A.X, Ras$^{G12D/T35S}$ plasmid + pEGFP-H2A.X, or Ras$^{G12D/T35S}$ plasmid + pEGFP-H2A.X ^{Y39A}, respectively. (B) These genes' transcription was examined through ChIP assay after transfection with pEGFP-H2A.X, or Ras$^{G12D/T35S}$ plasmid + pEGFP-H2A.X. $*p < .05$, $**p < .01$, GFP + H2A.X versus Ras + H2A.X, Ras + H2A.X versus Ras + H2A.X^{Y39A}, $***p < .001$ ($n = 3$).
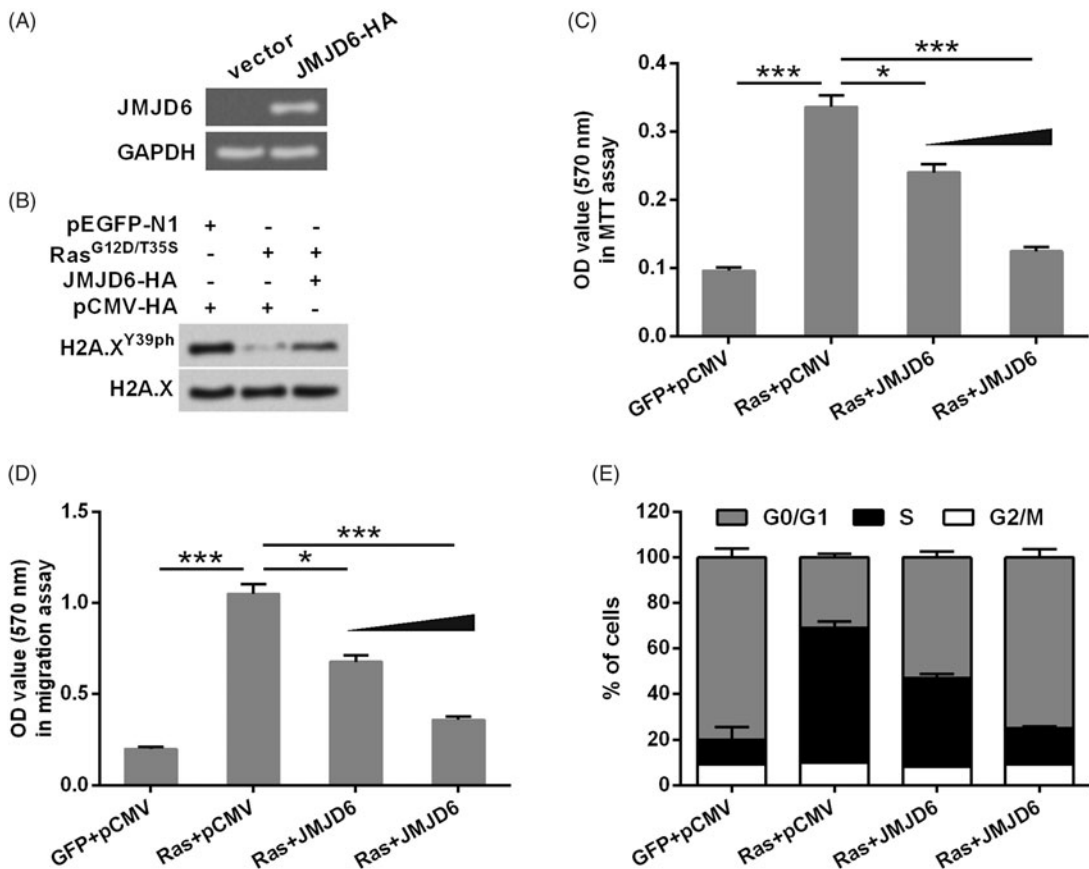
Figure 4. Overexpression of JMJD6 recovered H2A.X^{Y39ph} expression and uveal melanoma cell phenotypes. (A) JMJD6-HA (a HA-tagged plasmid for expression of JMJD6) or an empty vector was transfected into MP65 cells. Gel electrophoresis showed the mRNA level of JMJD6. (B) Ras$^{G12D/T35S}$ plasmid, JMJD6-HA, or empty vector was transfected into MP65 cells. The expression of H2A.X^{Y39ph} was examined through Western blot. (C) Cell activity was examined through MTT experiment. (D) Colonies numbers were measured through soft-agar colony formation experiment, and (E) cell cycle progression tested through flow cytometry were done after transfection with Ras$^{G12D/T35S}$ plasmid, JMJD6-HA (with raising concentrations, i.e. 0.5 and 1 g), or empty vector. $*p < .05$, $***p < .001$ ($n = 3$).

activation induced the up-regulation of MDM2 and down-regulation of H2A.X^{Y39ph}. Interestingly, the effects of ERK1/2 activation on H2A.X^{Y39ph} expression was abolished when MDM2 was silenced (Figure 6G). The efficiency of siRNA transfection was shown in Figure 6(F). All in all, these findings suggested that Ras-ERK1/2 signalling suppressed H2A.X phosphorylation probably through MDM2-mediated degradation of JMJD6.
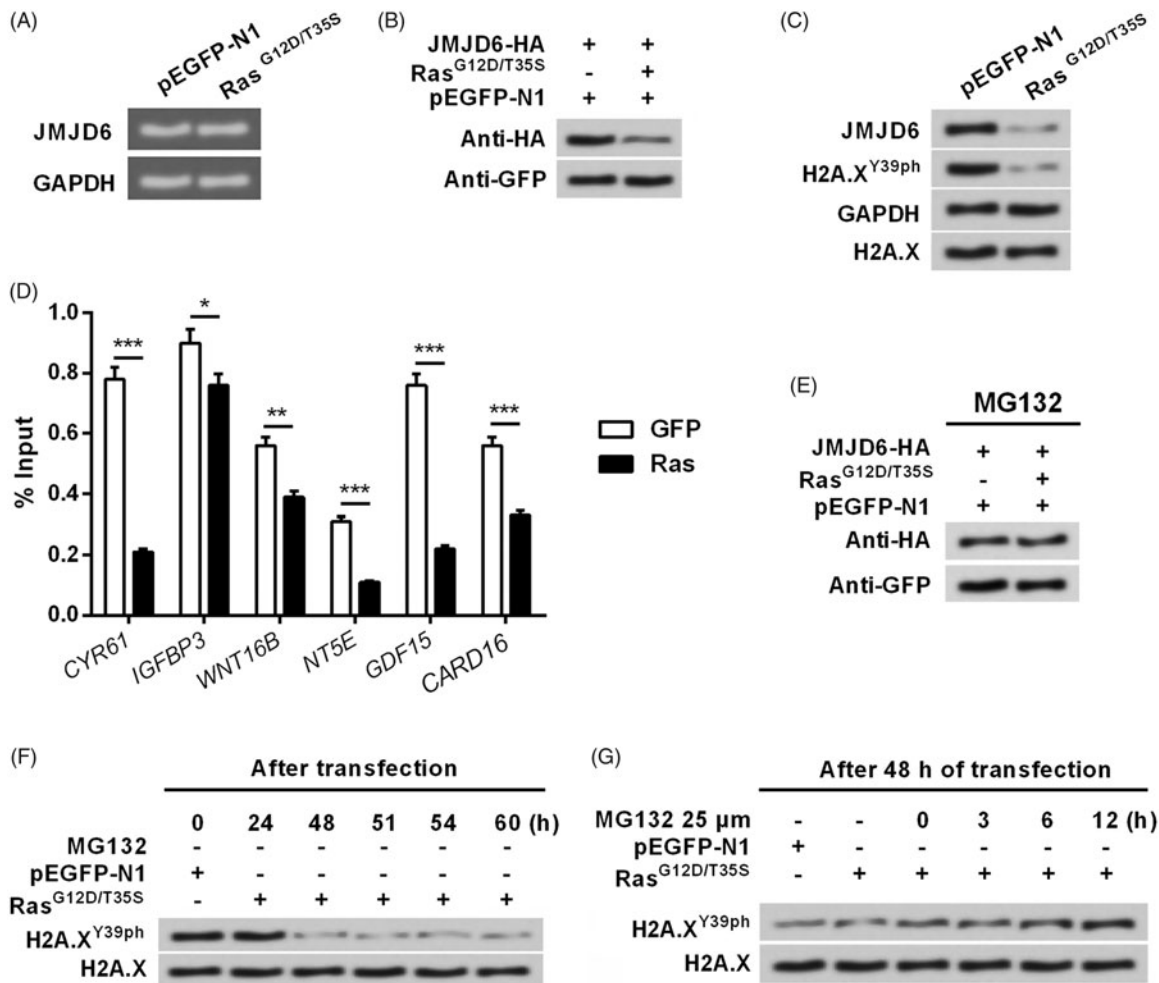
Figure 5. Activation of ERK1/2 induced the degradation of JMJD6 and led to the down-regulation of H2A.X^{Y39ph}. (A) Ras$^{G12D/T35S}$ plasmid or an empty vector was transfected into MP65 cells. Gel electrophoresis showed the mRNA level of JMJD6. (B) MP65 cells were transfected with JMJD6-HA, Ras$^{G12D/T35S}$ plasmid or empty vector. JMJD6 expression was examined through Western blot. (C) Ras$^{G12D/T35S}$ plasmid or an empty vector was transfected into MP65 cells. Protein levels of JMJD6 and H2A.X^{Y39ph} were examined through Western blot analysis. (D) If JMJD6 bind with the promoter of ERK1/2 downstream genes was examined through ChIP experiment. (E) JMJD6 expression was measured through Western blot after treating with MG132. (F) H2A.X^{Y39ph} expression was measured through Western blot after 0–60 h transfection. (G) H2A.X^{Y39ph} expression was examined through Western blot after treating with MG132 for 0–12 h. $^*p<.05$, $^{**}p<.01$, GFP versus Ras, $^{***}p<.001$ ($n=3$).

An explanation of how Ras-ERK1/2 and JMJD6-MDM2 regulate H2A.X^{Y39ph}

Figure 7 revealed the mechanism of how Ras-ERK1/2 and JMJD6-MDM2 regulate H2A.X^{Y39ph}. Ras point mutations activated ERK1/2 signalling, which inhibited H2A.X phosphorylation at Y39, leading to the uncontrolled growth and migration of uveal melanoma cells. Besides, ERK1/2 activation remarkably down-regulated the pro-transcriptional protein level of JMJD6, suggesting that Ras-ERK1/2 signalling inhibited H2A.X^{Y39ph} via post-transcriptional regulation of JMJD6. Additionally, ERK1/2 activation induced the up-regulation of MDM2, which reduced the expression of JMJD6. Taken together, Ras-ERK1/2 signalling restrained H2A.X^{Y39ph} possibly through MDM2-mediated degradation of JMJD6.

Discussion

It is well-known that histone modification is one of the main events driven the onset and maintenance of cancers. H2A.X phosphorylation is closely associated with DNA damage. And if not repaired correctly, DNA damage elevates genomically unstable, which initiates carcinogenesis and finally promoting the formation of cancer [17]. The C-terminus of H2A.X can phosphorylate in T136, S139 and Y142. Among which, S139 phosphorylation is considered an essential key signal for the recruitment and reservation of DNA damage response (DDR) complexes [18]. Interestingly, H2A.X phosphorylation at Y39 is a prerequisite for γ-H2A.X formation [8]. Besides, the potential involvement of H2A.X^{Y39ph} in cancer progression has been mentioned by Liu et al., who demonstrated that H2A.X^{Y39ph} was correlated with histological grade, tumour size, tumour node and survival rate of patients [8]. This work attempted to study the role of H2A.X^{Y39ph} in uveal melanoma MP65 cells growth and migration. As a result, we found that H2A.X^{Y39ph} could be notably down-regulated through ERK1/2 actuation. Silence of H2A.X^{Y39ph} contributed to the regulation of MP65 cells growth, migration and ERK1/2 downstream genes' transcription, like CYR61, IGFBP3, WNT16B, NT5E, GDF15 and CARD16. Furthermore, we found that Ras-ERK1/2 signalling repressed H2A.X phosphorylation might be through MDM2-mediated JMJD6 degradation.
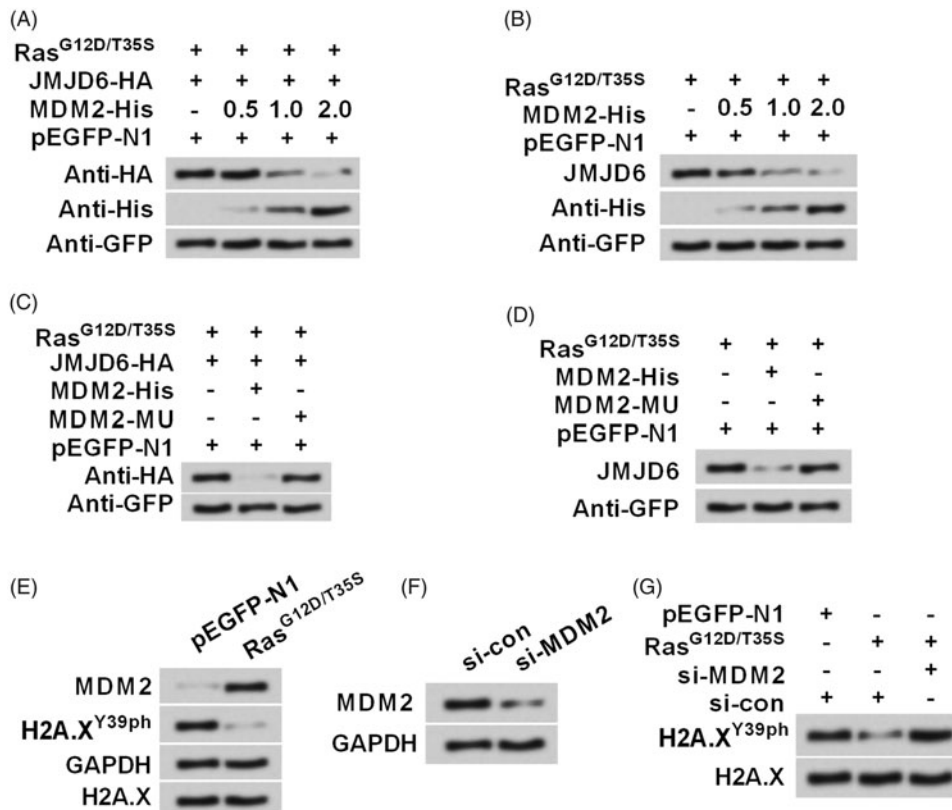
Figure 6. Activation of ERK1/2 degraded JMJD6 via modulating MDM2. Ras[G12D/T35S], JMJD6-HA, MDM2-His (a His-tagged plasmid for expression of MDM2), or empty vector was transfected into MP65 cells. (A) Exogenous and (B) endogenous expression of JMJD6 was examined through Western blot. MDM2-His was treated with increasing concentrations (0.5, 1.0 and 2.0 g). Subsequently, MDM2-His or MDM2-MU (the mutated MDM2) were transfected into cell and the (C) exogenous and (D) endogenous expression of JMJD6 was measured through Western blot. (E) The expression of MDM2 and H2A.X[Y39ph] were examined after transfection. (F) siRNA transfection was done to repress MDM2 expression. (G) The expression changes of H2A.X[Y39ph] were tested when MDM2 was silenced. All protein levels were tested by Western blot analysis.
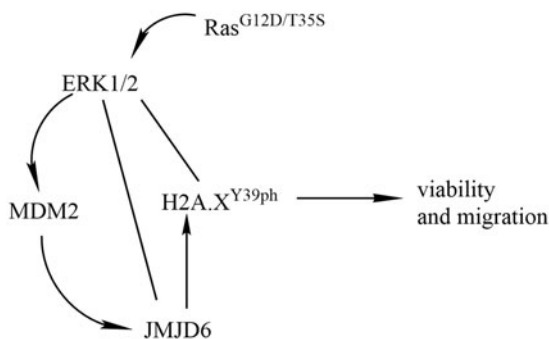
Figure 7. Diagram was made to explain how Ras-ERK1/2 and JMJD6-MDM2 regulate H2A.X[Y39ph].

ERK signalling pathway exists in all types of eukaryotic cells and participates in regulating cell proliferation, differentiation, apoptosis, metastasis and metabolism in multiple cancers, including uveal melanoma [19]. Ras is a switch of ERK signalling that Ras can active ERK signalling. In uveal melanoma, Ras-ERK signalling is often activated by genetic alterations [3,20], and it has been believed that activation of this signalling cascades led to the dysregulated tumour cells phenotype. Ras gene family has three members: HRas, NRas and KRas. In this study, we found that KRas mutated at G12D and T35S induced activation of ERK1/2, which were consistent with previous findings [15,16]. More interestingly, we found that Ras mutation inhibited the phosphorylation of

H2A.X at Y39. Our consequents revealed that Ras-mediated ERK1/2 actuation could repress the phosphorylation of H2A.X at Y39. Besides, based on these findings, we inferred that H2A.X[Y39ph] might contribute to the onset and maintenance of uveal melanoma.

H2A.X was considered as exerting tumour suppressive roles and is considered as a biomarker for drug response [21]. In triple-negative breast cancer and melanoma, S139 phosphorylation of H2A.X was occurred and was correlated with poor prognosis [22–24]. Also, γ-H2AX has been mentioned as a forecasted biomarker for hepatocellular carcinoma risk for in preneoplastic lesions [25]. In this study, H2A.X[Y39A] (a mimicked plasmid for expression of H2A.X[Y39ph]) was found to inhibit MP65 cells viability, migration and colony formation capacity, suggesting the anti-tumour effects of H2A.X[Y39ph] on uveal melanoma. Our findings suggested a potentially promising approach for uveal melanoma treatment.

CYR61 is a connective tissue growth factor which has been considered as a crucial mediator in the developing and metastasis of cancers [26]. High expression of CYR61 was present in cervical cancer [27] and oesophageal squamous cell carcinoma [28], and exerted diverse functions in several types of cancers [29]. In malignant melanoma, CYR61 worked as a biomarker for tumour cells proliferation and metastasis, making it a potential target for melanoma treatment [30]. Apart from CYR61, IGFBP3 [31], WNT16B [32], NT5E [33], GDF15 [34]

and CARD16 [35] have been demonstrated as tumour-relevant genes (tumour-promoter or tumour-suppressor) in some cancers. By performing qRT-PCR, CYR61, IGFBP3 and WNT16B were negatively regulated, while NT5E, GDF15 and CARD16 were positively regulated through H2A.X^{Y39ph}. Besides, ChIP assay results implied that ERK1/2 downstream genes' transcription which was closely associated with tumour progression could be regulated by H2A.X^{Y39ph}. These findings further confirmed the involvement of H2A.X^{Y39ph} in uveal melanoma cells growth and migration.

JMJD6 is a well-known protease for mediation of histone modification. A previous study has mentioned that JMJD6 could regulate H2A.X phosphorylation, and inhibited the triple-negative breast cancer cells growth [12]. Consistently, we found that H2A.X^{Y39ph} expression was suppressed by ERK1/2, however, JMJD6 recovered H2A.X^{Y39ph} expression to exert the effect of H2A.X^{Y39ph} on inhibiting MP65 cells growth and migration. Our study further showed that JMJD6 could be degraded by MDM2. As a chromatin modifier, MDM2 is capable of interacting with the MRN complex and thus functions as a key mediator in DNA repair [36]. MDM2 is reported to directly interact with histones and ubiquitinate histone H2A [37]. What is more, MDM2 plays repressing roles in several genes' expression, such as p53, which explains its tumour-promoting effects [38]. According to these evidences, Ras-ERK1/2 signalling repressed H2A.X phosphorylation to play tumour-promoting function possibly through MDM2-mediated degradation of JMJD6.

In conclusion, this study tried to use epigenetics to explain the tumour-promoting function Ras-ERK1/2 signalling in uveal melanoma, suggesting the potential role of Ras-ERK1/2 signalling in monitoring uveal melanoma. Besides, Ras-ERK1/2 signalling suppressed H2A.X phosphorylation at Y39, which led to the promotion of uveal melanoma development. Phosphorylation of H2A.X was mediated possibly through JMJD6 which could be degraded by MDM2. The regulatory principle of Ras-ERK1/2 signalling in H2A.X^{Y39ph} may offer a latent epigenetic target in uveal melanoma treatment.

Data availability

The datasets used and/or analyzed during the current study are available from the corresponding author on reasonable request.

Disclosure statement

The authors declare that they have no conflict of interest.

Funding

ORCID

Weixuan Sun 🔟 http://orcid.org/0000-0003-4615-8463

References

[1] Wang YC, Yang X, Wei WB, et al. Role of microRNA-21 in uveal melanoma cell invasion and metastasis by regulating p53 and its downstream protein. Int J Ophthalmol. 2018;11(8):1258–1268.

[2] Board PDQATE. Intraocular (uveal) melanoma treatment (PDQ(R)): health professional version. PDQ cancer information summaries. Bethesda (MD): National Cancer Institute (US); 2002.

[3] Van Raamsdonk CD, Griewank KG, Crosby MB, et al. Mutations in GNA11 in uveal melanoma. N Engl J Med. 2010;363(23):2191–2199.

[4] Chua V, Aplin AE. Novel therapeutic strategies and targets in advanced uveal melanoma. Curr Opin Oncol. 2018;30(2):134–141.

[5] Orenay-Boyacioglu S, Kasap E. Expression profiles of histone modification genes in gastric cancer progression. Mol Biol Rep. 2018;45:2275–2282.

[6] Redon CE, Nakamura AJ, Martin OA, et al. Recent developments in the use of gamma-H2AX as a quantitative DNA double-strand break biomarker. Aging. 2011;3(2):168–174.

[7] Baltanas FC, Weruaga E, Valero J, et al. Albumin attenuates DNA damage in primary-cultured neurons. Neurosci Lett. 2009;450(1):23–26.

[8] Liu Y, Long YH, Wang SQ, et al. Phosphorylation of H2A.X(T)(yr39) positively regulates DNA damage response and is linked to cancer progression. FEBS J. 2016;283(24):4462–4473.

[9] Bonner WM, Redon CE, Dickey JS, et al. GammaH2AX and cancer. Nat Rev Cancer. 2008;8(12):957–967.

[10] Georgoulis A, Vorgias CE, Chrousos GP, et al. Genome instability and gammaH2AX. Int J Mol Sci. 2017;18(9):1979.

[11] Poulard C, Rambaud J, Lavergne E, et al. Role of JMJD6 in breast tumourigenesis. PLOS One. 2015;10(5):e0126181.

[12] Liu Y, Long YH, Wang SQ, et al. JMJD6 regulates histone H2A.X phosphorylation and promotes autophagy in triple-negative breast cancer cells via a novel tyrosine kinase activity. Oncogene. 2018;38:980–997.

[13] Livak KJ, Schmittgen TD. Analysis of relative gene expression data using real-time quantitative PCR and the 2(-Delta Delta C(T)) method. Methods. 2001;25(4):402–408.

[14] Liu Y, Xing ZB, Zhang JH, et al. Akt kinase targets the association of CBP with histone H3 to regulate the acetylation of lysine K18. FEBS Lett. 2013;587(7):847–853.

[15] Janssen RA, Veenstra KG, Jonasch P, et al. Ras- and Raf-induced down-modulation of non-muscle tropomyosin are MEK-independent. J Biol Chem. 1998;273(48):32182–32186.

[16] Kidger AM, Sipthorp J, Cook SJ. ERK1/2 inhibitors: new weapons to inhibit the RAS-regulated RAF-MEK1/2-ERK1/2 pathway. Pharmacol Ther. 2018;187:45–60.

[17] Negrini S, Gorgoulis VG, Halazonetis TD. Genomic instability–an evolving hallmark of cancer. Nat Rev Mol Cell Biol. 2010;11(3):220–228.

[18] Bao Y. Chromatin response to DNA double-strand break damage. Epigenomics. 2011;3(3):307–321.

[19] Babchia N, Calipel A, Mouriaux F, et al. The PI3K/Akt and mTOR/P70S6K signaling pathways in human uveal melanoma cells: interaction with B-Raf/ERK. Invest Ophthalmol Vis Sci. 2010;51(1):421–429.

[20] Van Raamsdonk CD, Bezrookove V, Green G, et al. Frequent somatic mutations of GNAQ in uveal melanoma and blue naevi. Nature. 2009;457(7229):599–602.

[21] Corujo D, Buschbeck M. Post-translational modifications of H2A histone variants and their role in cancer. Cancers. 2018;10(3):59.

[22] Nagelkerke A, van Kuijk SJ, Sweep FC, et al. Constitutive expression of gamma-H2AX has prognostic relevance in triple negative breast cancer. Radiother Oncol. 2011;101(1):39–45.

[23] Warters RL, Adamson PJ, Pond CD, et al. Melanoma cells express elevated levels of phosphorylated histone H2AX foci. J Invest Dermatol. 2005;124(4):807–817.

[24] Wasco MJ, Pu RT, Yu L, et al. Expression of gamma-H2AX in melanocytic lesions. Hum Pathol. 2008;39(11):1614–1620.

[25] Matsuda Y, Wakai T, Kubota M, et al. DNA damage sensor gamma -H2AX is increased in preneoplastic lesions of hepatocellular carcinoma. ScientificWorldJournal. 2013;2013:1.

[26] Nguyen LT, Song YW, Cho SK. Baicalein inhibits epithelial to mesenchymal transition via downregulation of Cyr61 and LOXL-2 in MDA-MB231 breast cancer cells. Mol Cells. 2016;39(12): 909–914.

[27] Mayer S, Gabriel B, Erbes T, et al. Cyr61 expression pattern and association with clinicopathological factors in patients with cervical cancer. Anticancer Res. 2017;37(5):2451–2456.

[28] Wang P, Li L, Li T. Positive correlation of cysteine-rich 61 and target genes of Wnt/beta-catenin pathway in esophageal squamous cell carcinoma. J Can Res Ther. 2016;12:19–22.

[29] Niu CC, Zhao C, Yang Z, et al. Inhibiting CCN1 blocks AML cell growth by disrupting the MEK/ERK pathway. Cancer Cell Int. 2014;14(1):74.

[30] Chen J, Liu Y, Sun Q, et al. CYR61 suppresses growth of human malignant melanoma. Oncol Rep. 2016;36(5):2697–2704.

[31] Ho GYF, Zheng SL, Cushman M, et al. Associations of insulin and IGFBP-3 with lung cancer susceptibility in current smokers. J Natl Cancer Inst. 2016;108(7):djw012.

[32] Johnson LM, Price DK, Figg WD. Treatment-induced secretion of WNT16B promotes tumor growth and acquired resistance to chemotherapy: implications for potential use of inhibitors in cancer treatment. Cancer Biol Ther. 2013;14(2):90–91.

[33] Peng D, Hu Z, Wei X, et al. NT5E inhibition suppresses the growth of sunitinib-resistant cells and EMT course and AKT/GSK-3beta signaling pathway in renal cell cancer. IUBMB Life. 2018;71: 113–124.

[34] Zhang Y, Wang X, Zhang M, et al. GPF15 promotes epithelial-to-mesenchymal transition in colorectal carcinoma. Artif Cells Nanomed Biotechnol. 2018;46:652–658.

[35] Karasawa T, Kawashima A, Usui F, et al. Oligomerized CARD16 promotes caspase-1 assembly and IL-1beta processing. FEBS Open Biol. 2015;5(1):348–356.

[36] Wienken M, Moll UM, Dobbelstein M. Mdm2 as a chromatin modifier. J Mol Cell Biol. 2017;9(1):74–80.

[37] Minsky N, Oren M. The RING domain of Mdm2 mediates histone ubiquitylation and transcriptional repression. Mol Cell. 2004;16(4): 631–639.

[38] Feeley KP, Adams CM, Mitra R, et al. Mdm2 is required for survival and growth of p53-deficient cancer cells. Cancer Res. 2017;77(14): 3823–3833.